Ultrafast relaxation dynamics of spin density wave order in BaFe$_2$As$_2$ under high pressures

Ivan Fotev [1,2] Stephan Winnerl,[1] Saicharan Aswartham [3] Sabine Wurmehl,[3,4] Bernd Büchner,[3,4] Harald Schneider,[1] Manfred Helm,[1,2] and Alexej Pashkin [1,*]

[1]*Helmholtz-Zentrum Dresden-Rossendorf, 01328 Dresden, Germany*
[2]*Technische Universität Dresden, 01062 Dresden, Germany*
[3]*Leibniz IFW Dresden, 01069 Dresden, Germany*
[4]*Institute of Solid State and Materials Physics and Würzburg-Dresden Cluster of Excellence ct.qmat,
Technische Universität Dresden, 01062 Dresden, Germany*

BaFe$_2$As$_2$ is the parent compound for a family of iron-based high-temperature superconductors as well as a prototypical example of the spin density wave (SDW) system. In this study, we perform an optical pump-probe study of this compound to systematically investigate the SDW order across the pressure-temperature phase diagram. The suppression of the SDW order by pressure manifests itself through the increase of relaxation time together with the decrease of the pump-probe signal and the pump energy necessary for complete vaporization of the SDW condensate. We have found that the pressure-driven suppression of the SDW order at low temperature occurs gradually, in contrast to the thermally induced SDW transition. Our results suggest that the pressure-driven quantum phase transition in BaFe$_2$As$_2$ (and probably other iron pnictides) is continuous and it is caused by the gradual worsening of the Fermi-surface nesting conditions.

I. INTRODUCTION

Iron pnictide high-T_c superconductors have become one of the most intensively studied material systems since their discovery in 2008 [1]. In contrast to superconducting cuprates, they demonstrate a high sensitivity to applied stress, for instance, to hydrostatic pressure. The magnetic spin density wave (SDW) order in a parental compound for these materials can be suppressed not only by chemical doping but also by pressure [2]. Moreover, since parental iron pnictides are metallic even in the absence of doping, they can undergo pressure-induced SDW-to-superconductor quantum phase transition (QPT) at low temperatures [3,4]. Exploring the mechanism of this transition, the competition and coexistence of the magnetic order and the superconducting condensate are crucial for the understanding of high-T_c superconductivity in iron pnictides.

For the present study we have chosen BaFe$_2$As$_2$ as a prime example of a well-known parental iron pnictide compound, in which the electronic state can be controlled by external pressure. At ambient pressure the onset of the magnetic SDW order occurs simultaneously with the structural transition from the tetragonal to orthorhombic phase at $T_{SDW} = 137$ K [5]. Chemical doping or an external pressure application causes a decrease of the transition temperature T_{SDW} [6]. The p-T phase diagram of BaFe$_2$As$_2$ depicted in Fig. 1 is qualitatively similar to that of chemically doped compounds: at low temperatures the system is in the SDW state that is gradually suppressed by increasing the doping level or pressure until superconductivity (SC) sets in [7]. Upon applying

high pressures, the structural properties of BaFe$_2$As$_2$ change the same way as in the chemically doped materials [2]. The structural changes are correlated with the reduction of the Fermi-surface nesting between the inner hole and electron pockets, which results in SDW state suppression above a pressure of $\approx$3 GPa (depending on the experimental conditions) [2,3,8]. This suppression results in quantum critical behavior [9], indicating that the pressure- or doping-driven SDW phase transition should be second order, in contrast to the first-order temperature-induced SDW transition [10].

Measuring the pressure dependence of the SDW or superconducting energy gaps poses a significant challenge because it has to be performed on a sample inside a diamond anvil cell (DAC). This precludes the use of angle-resolved photoemission spectroscopy (ARPES), which requires direct access to the sample's surface in vacuum. Tunneling spectroscopy under high pressures was demonstrated for conventional superconductors [12]. However, it has not been applied to high-T_c iron-based superconductors yet. Nevertheless, a recent tunneling spectroscopy study demonstrated a strong impact of the local surface strain on the superconducting gap in LiFeAs [13]. Up to now, the SDW and the superconducting energy gaps in BaFe$_2$As$_2$ under high pressure have been determined using infrared spectroscopy [14]. Reference [14] revealed the coexistence of the SDW and SC orders at 3.6 GPa since the spectral weight of the SDW gap excitation is not significantly affected by the emergence of the superconductivity.

In addition to infrared spectroscopy, which probes the linear optical response of a material, nonlinear pump-probe spectroscopy provides another way to estimate the energy gaps in high-T_c superconductors via the analysis of quasiparticle relaxation dynamics [15]. The main advantage of pump-probe spectroscopy is its high sensitivity to the
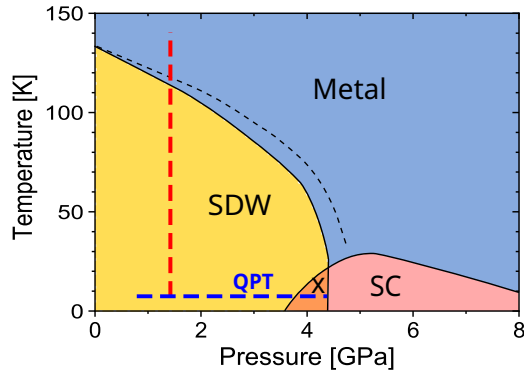
FIG. 1. Schematic pressure-temperature phase diagram of $BaFe_2As_2$, mostly according to [3]. The black dashed line denotes the structural phase transition that splits out of the SDW transition with doping [6] or pressure [11]. Dashed red and blue lines illustrate $p = const$ and $T = const$ measurement trajectories corresponding to measurements shown in Figs. 2 and 5, respectively.
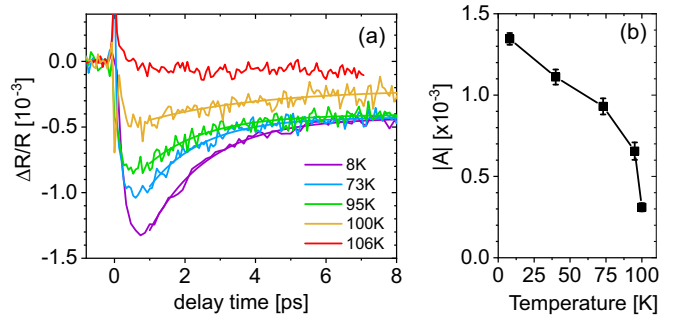

FIG. 2. (a) Relative differential reflectivity transients and their monoexponential fits, recorded at $p = 1.4$ GPa for several temperatures and fixed pump fluence of $75\,\mu J/cm^2$. (b) Amplitude of the exponential decay process as a function of temperature. The substantial drop in amplitude above 100 K, reveals the phase transition from the SDW to the metallic state.

evolution of electronic order in close vicinity to phase transitions. Numerous pump-probe spectroscopy studies of iron pnictides have demonstrated that the suppression of the SDW or SC order around the transition temperatures is accompanied by a critical slowing down of the relaxation dynamics for the given electronic order [16–18]. Near-infrared-pump–midinfrared-probe spectroscopy of parental $BaFe_2As_2$ showed that the coherent lattice oscillation that modulates the Fe-As-Fe bonding angle can periodically induce transient SDW ordering, even at temperatures above T_{SDW} [19].

Here we report a study of the SDW order in $BaFe_2As_2$ across the p-T phase diagram. Our results demonstrate a critical slowing down of the SDW relaxation time caused by the suppression of SDW order by temperature or pressure. However, in contrast to the abrupt change across the temperature-driven first-order transition, the increase in the relaxation time caused by pressure at 8 K is gradual, indicating the second-order character of the quantum phase transition.

II. EXPERIMENTAL RESULTS

A. Sample preparation and experimental setup

The studied $BaFe_2As_2$ monocrystals were grown by a self-flux high-temperature solution growth technique [5,20]. The sample, $100 \times 85\,\mu m^2$ in size and about $30\,\mu m$ thick, was initially cleaved from the $BaFe_2As_2$ monocrystal, so that it could fit into the sample chamber of the DAC. The commercial closed-cycle cryostat system with integrated DAC (Diacell CCS-DAC from Almax easyLab) enabled us to perform *in situ* control of pressure and temperature independently due to the gas membrane-driven DAC system. A Ti:sapphire amplifier system operating at a repetition rate of 250 kHz generated the 60 fs long laser pulses utilized in the experiment. The pump and the probe beams (both with a wavelength of 800 nm) were focused onto the sample inside the DAC, and the reflected probe signal was collected using a confocal microscopy scheme. A ruby chip was placed inside the sample chamber, next to the sample, and used for external pressure calibration [21]. We chose CsI powder as the

pressure-transmitting medium in order to ensure direct contact between the sample and the diamond anvil.

B. Temperature dependence at fixed pressure

Figure 2(a) shows a set of photoinduced differential reflectivity $\Delta R(t)/R$ measurements, obtained at a pump fluence of $F = 75\,\mu J/cm^2$ and fixed pressure of 1.4 GPa. Together these measurement points correspond to the vertical path in the p-T diagram, marked by the dashed red line in Fig. 1. At lower temperatures $BaFe_2As_2$ is in the SDW phase, and the photoinduced reflectivity change $\Delta R/R$ reaches its negative maximum quickly after the photoexcitation at the zero delay time. Then, the signal decays within a few picoseconds to a nearly constant level corresponding to a thermalized hot state. We assign this monoexponential, fast-decaying part of the signal to the relaxation of the SDW phase. Its amplitude $|A|$ is proportional to the concentration of photoexcited quasiparticles: $|A| \propto n_{pe}$ [22–24]. With increasing temperature A decreases substantially, and near 100 K the relaxation process slows down. Finally, the pump-probe response at $T = 106$ K (red line) does not contain the SDW relaxation signature anymore and demonstrates only a small signal with opposite sign with a much faster decay. We assign it to the hot-electron cooling process typical for metals.

Figure 2(b) shows the temperature dependence of the exponential decay amplitude. Its strong drop around 100 K is related to the SDW phase transition to the nonmagnetic metallic phase. Naturally, this transition temperature determined for a pressure of 1.4 GPa is lower than $T_{SDW} = 137$ K at atmospheric pressure. Simultaneously, we observe indications of the critical slowing down of the relaxation dynamics that was previously reported for SmFeAsO [18], $SrFe_2As_2$ [17], and $BaFe_2As_2$ [16,25]. However, it was not possible to reliably quantify this effect since close to T_{SDW}, where the slowdown is expected, the signal amplitude becomes very small and the fitting uncertainty is too large.

At temperatures well below T_{SDW} the relaxation time $\tau \approx 1.6$ ps remains nearly constant. This behavior contradicts the bimolecular recombination model: $dn_{pe}/dt = -2Rn_Tn_{pe} - Rn_{pe}^2$, where R is the bimolecular recombination
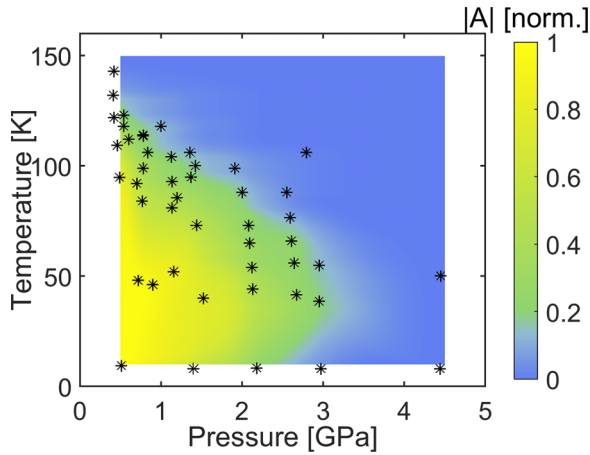
FIG. 3. *p-T* diagram obtained from the amplitudes of the SDW transients *A*. At the phase transitions to metallic or superconducting states the amplitude goes to zero (blue). The individual measurement points are represented by asterisks. The color map is obtained by linear interpolation and subsequent smoothing.

coefficient and n_T and n_{pe} are the densities of thermally and photoexcited quasiparticles, respectively. Here the first term, $Rn_T n_{pe}$, corresponds to the recombination of a photoexcited quasiparticle with a thermally populated one, and the second term, Rn_{pe}^2, represents the recombination of the two photoexcited quasiparticles [26]. At low temperatures the bimolecular model predicts that the initial recombination rate τ^{-1} should increase with n_T, which strongly depends on temperature. Similar to our observations, studies on SmFeAsO [18] and SrFe$_2$As$_2$ [17] also reported τ that does not increase with decreasing temperatures. This was interpreted as a hint of an additional relaxation channel besides the bimolecular recombination at the SDW gap, namely, an interband scattering of quasiparticles to other, ungapped electronic bands [17]. Such scattering should be temperature independent, and it should result in an additional, dominating monomolecular recombination term, $-n_{pe}/\tau$, in the rate equation.

C. Suppression of the SDW relaxation by pressure and temperature

The data from all temperature-dependent measurements at fixed pressures from 0.5 to 4.4 GPa (vertical scans of the *p-T* diagram) are combined in a *p-T* diagram, depicted in Fig. 3. The color represents the amplitude of the normalized monoexponential signal $|A|$: from yellow for 1 to blue for 0. Therefore, the metallic phase corresponds to the blue region of the diagram, and the density of the SDW condensate is displayed by the brightness of the yellow color. As expected from Fig. 1, the temperature at which the amplitude vanishes, i.e., the SDW transition temperature $T_{SDW}(p)$, decreases with pressure, and at high pressures the SDW state gets completely suppressed. From the 4.4 GPa measurements we could not identify SDW $\Delta R(t)/R$ transients anymore, so we assigned zeros to the amplitude of those points.

As shown in Figs. 2(b) and 3, with increasing temperature the amplitudes smoothly and monotonically approach zero at the corresponding $T_{SDW}(p)$ for each pressure, which was
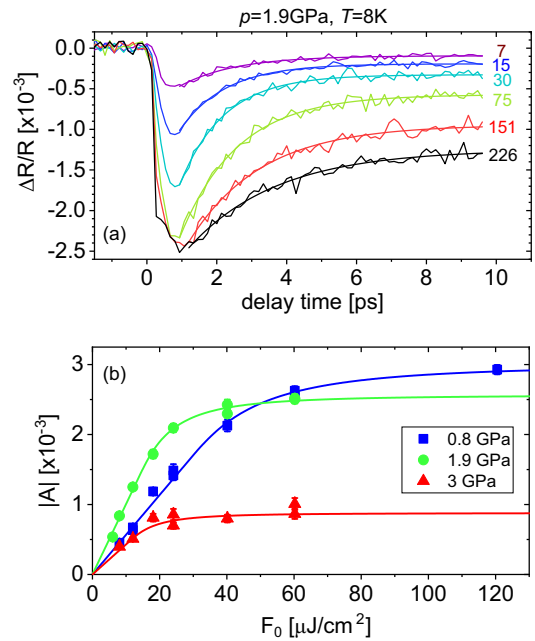

FIG. 4. (a) Reflectivity changes $\Delta R(t)/R$ measured at 1.9 GPa and 8 K for selected pump fluences. The fluence values are given in microjoules per square centimeter. (b) Fluence dependence of the SDW reflectivity transient amplitudes $|A|$ for several pressures. F_0 is the part of the pump fluence F which penetrates into the sample, after the reflection from its surface. Lines are the fits with the model of the threshold fluence for condensate vaporization from [28].

also reported in Ref. [16]. This is in contrast to two other studies on iron pnictides [17,18], in which the temperature dependence of $A(T)$ exhibits a small increase relatively close to T_{SDW} before starting to drop rapidly: a characteristic feature of the bottleneck model [27]. However, the pump fluences used in the present study are much larger than in the other three reports, making the direct comparison harder.

D. Relaxation dynamics and its fluence dependence at 8 K

Now let us examine the suppression of the SDW order by pressure in the ground state, i.e., the path of the quantum phase transition as it is depicted in Fig. 1. In order to gain more reliable information about the SDW phase we measured the pump-probe response for various pump fluences at each pressure in the range from 0.8 to 3 GPa. Figure 4(a) presents a set of measurements taken at different pump fluences at a pressure of 1.9 GPa and temperature of 8 K. Starting at $7\,\mu J/cm^2$, the amplitude A grows linearly with pump fluence F, roughly up to $30\,\mu J/cm^2$, after which it completely saturates. This happens because the proportionality between the number of photoexcited quasiparticles and the number of pump photons $n_{pe} \propto F$, which is valid in the low-fluence regime, breaks down when the pump fluence becomes high enough for a noticeable depletion of the SDW condensate. Finally, at a certain threshold vaporization fluence F_T the SDW condensate is completely suppressed, and consequentially, no more quasiparticles can be excited. As a result, n_{pe} and the pump-probe signal A get saturated.
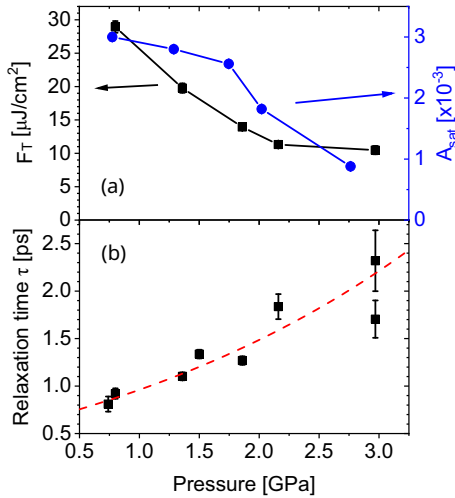
FIG. 5. (a) Pressure dependence of the threshold vaporization fluence F_T (black squares) and saturation amplitudes (blue circles). The value of F_T can be considered the measure of SDW condensation energy. (b) Pressure dependence of the relaxation time $\tau(p)$ at fixed temperature $T = 8$ K and fluence of 30 μJ/cm^2.

The saturation curves measured at a few chosen pressures are shown in Fig. 4(b). Here $F_0 = (1 - R)F$ is the part of the pump fluence F which penetrates the sample after the reflection from its surface. $R = 0.2$ is the reflectivity of BaFe$_2$As$_2$ (at 800 nm) with respect to the diamond, which is almost independent of pressure and temperature [14]. Although the curves look qualitatively similar, the saturation fluence F_T and the saturation amplitude A_{sat} decrease with pressure. We extracted both parameters from the fits based on the model introduced in Ref. [28], which takes into account the lateral Gaussian and exponential depth profiles of the pump and probe beams. The fitting curves are represented by lines in Fig. 4(b). The obtained values of $F_T(p)$ and $A_{sat}(p)$ for all measured pressures are presented in Fig. 5(a) with black squares and blue circles, respectively.

Besides the suppression of the pump-probe signal and the decrease of the saturation fluence, the applied pressure also affects the relaxation time τ. Figure 5(b) shows its pressure dependence $\tau(p)$ for a fixed $T = 8$ K and $F = 30$ μJ/cm^2. Similar to the temperature-dependent measurements [16,25], the increasing τ signals the vicinity of the phase transition. As the system approaches the transition pressure, the gap $\Delta_{SDW}(p)$ gets smaller, and consequently, the SDW recovery time slows down. It is known that near the transition point the relaxation time is inversely proportional to the gap $\tau \propto \Delta^{-1}$ [15,29,30]. Thus, all these observations indicate the gradual suppression of the SDW state by the external pressure, leading to the quantum phase transition in BaFe$_2$As$_2$. Since at 4.4 GPa we do not observe any SDW relaxation signature (see the Supplemental Material [31]), the pressure of the QPT should be between 3 and 4.4 GPa.

III. DISCUSSION

Like in the case of the superconducting condensate in cuprates [28] it is useful to compare the energy deposited at the saturation fluence with the thermodynamical condensation

energy that can be obtained from the specific heat measurements [32]. For the lowest pressure measurement at $p = 0.8$ GPa the threshold fluence is $F_T = 29$ μJ/cm^2 [Fig. 5(a)]. In order to estimate the absorbed energy density we set the optical penetration depth of BaFe$_2$As$_2$ at 1.55 eV (800 nm) to be $\lambda_{op} = 36$ nm. This value is calculated using the reported real parts of dielectric constant $\varepsilon_1 \approx 1$ and optical conductivity $\sigma_1 = 1500$ Ω^{-1} cm^{-1} taken from Ref. [33]. Strictly speaking, the mentioned values of ε_1 and σ_1 were measured on the optimally doped compound, but since the reflectivity R is the same at 1.55 eV for the doped and parent compounds [34], we assume that it also holds for ε_1 and σ_1 and, consequently, λ_{op}. Therefore, the absorbed energy density at the vaporization threshold is $F_T/\lambda_{op} = 8$ J/cm^3. On the other hand, the thermodynamic SDW condensation energy is estimated to be $E_c/V = 1.6$ J/cm^3 using the specific heat $C(T)$ data for the parent BaFe$_2$As$_2$ ($p = 0$ GPa) [32]. Thus, the pump energy necessary for the vaporization of the SDW condensate is about 5 times larger than the condensation energy density of BaFe$_2$As$_2$. A similar result was reported for La$_{2-x}$Sr$_x$CuO$_4$ cuprate superconductors and was interpreted as evidence that a large portion of the pump energy goes to the phonon subsystem and does not affect the electronic condensate [28]. Therefore, the saturation amplitude A_{sat} that is related to the full depletion of the SDW condensate appears to be a more reliable parameter for estimating the SDW gap energy.

According to the Ginzburg-Landau theory, the order parameter scales as $|\Delta|^2 \propto n_{cond} \propto A_{sat}$ (n_{cond} is the condensate density) and $|\Delta| \propto 1/\tau$ when $T \to T_{SDW}$. Figure 6(a) shows the normalized $\sqrt{A(T)}$ dependence at 1.4 GPa and $F = 75$ μJ/cm^2 (blue squares). Based on the results in Fig. 5(a), this fluence value corresponds to the saturation regime, and thus, we expect that $|\Delta_{SDW}| \propto \sqrt{A}$. For comparison, Fig. 6(a) also shows the normalized SDW gap $\Delta_{SDW}(T)$ (gray triangles), extracted from the ARPES measurements [35]. Since, in contrast to the ARPES study, the depicted pump-probe results were recorded under high pressure ($p = 1.4$ GPa), the corresponding SDW transition temperatures are different: for our data $T_{SDW} \approx 100$ K, and for the ARPES study $T_{SDW} = 138$ K. In order to compare both data sets, the horizontal axis in Fig. 6(a) is normalized to T_{SDW}. They match quite well, demonstrating that the relation $|\Delta_{SDW}| \propto \sqrt{A_{sat}}$ is fulfilled for a broad range of temperatures below the SDW transition. Some deviation is observed far from the phase transition ($T < 0.3 T_{SDW}$) where the Ginzburg-Landau theory is no longer fully applicable.

Now we apply the same method to evaluate the SDW gap as a function of pressure. Figure 6(b) shows the pressure dependence of Δ_{SDW} at $T = 8$ K estimated as $\sqrt{A_{sat}(p)}$ using the saturation amplitude values from Fig. 5(a). In addition, the evaluated relaxation time $\tau(p)$ for $F = 30$ μJ/cm^2 [Fig. 5(b)] is reliable enough to use for another estimation of the SDW gap as $\Delta_{SDW} \propto 1/\tau(p)$, which is depicted in Fig. 6(b) as dark yellow circles. In general, all data in Fig. 6(b) indicate the trend of a *gradual* decrease of Δ_{SDW} by about 50% with the pressure increase up to 3 GPa. This corresponds to $p/p_{SDW} > 0.7$, taking into account that $p_{SDW} < 4.4$ GPa according to our results. If we compare Figs. 6(a) and 6(b), it is apparent that the phase transition achieved by increasing pressure happens much more gradually compared to the first-order
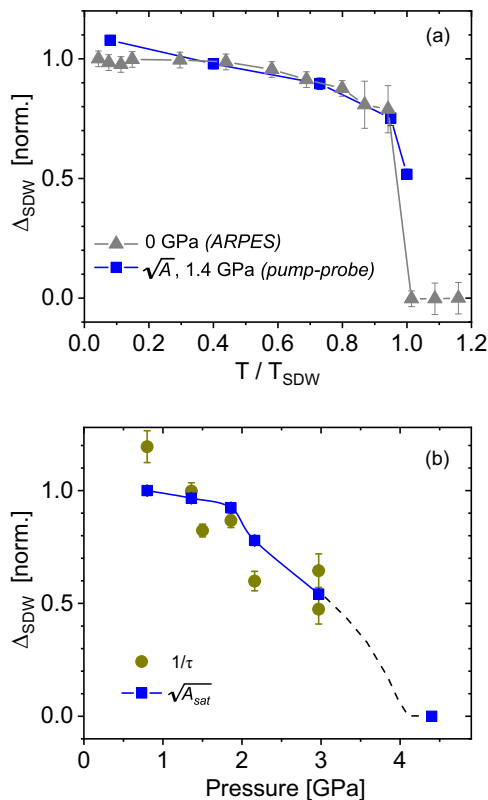
FIG. 6. (a) Temperature dependence of $\sqrt{A(T)}$ (blue squares) from the measurements at 1.4 GPa and $F = 75\,\mu J/cm^2$, compared with the $BaFe_2As_2$ SDW gap $\Delta_{SDW}(T)$ (gray triangles), extracted from the ARPES study at $p = 0$ GPa [35]. (b) The evolution of the SDW gap with pressure at $T = 10$ K estimated as $\sqrt{A_{sat}}$ and $1/\tau$. The highest pressure point shows the absence of the SDW order at 4.4 GPa. The dashed line schematically depicts the evolution of $\Delta_{SDW}(T)$ across the QPT.

thermally driven phase transition. Possibly, this indicates the second-order character of the pressure-induced QPT in $BaFe_2As_2$ that we schematically depict by the dashed line in Fig. 6(b). This conclusion agrees with the observation of quantum fluctuations near the quantum critical point in isovalently doped $BaFe_2(As_xP_{1-x})_2$ [9]. Microscopically, the gradual character of the pressure-induced changes can be understood as being the result of a gradual failure of the Fermi-surface nesting that causes the suppression of the SDW order [2].

Finally, we discuss the possible pressure-induced super-conducting phase. Our data demonstrate that for pressures well above 3 GPa the SDW order is fully suppressed, and according to the phase diagram (Fig. 1), we expect the onset of the superconductivity. In order to verify that, we measure pump-probe traces $\Delta R(t)/R$ at 8 K and 4.4 GPa (see the Supplemental Material). All pump-probe traces taken at various pump fluences show the same relaxation dynamics, which is much faster than in the SDW state. The absence of fluence-dependent relaxation dynamics and saturation behavior leads us to the conclusion that the fast dynamics observed at 4.4 GPa does not come from the superconducting or SDW state, but rather from the cooling of the hot electrons in the metallic phase.

IV. CONCLUSION

We performed a systematic temperature- and pressure-dependent pump-probe study in order to investigate the evolution of the SDW order in $BaFe_2As_2$. Measuring the amplitude of the relaxation process enabled us to construct the p-T phase diagram that depicts the variation of the SDW order across the whole range of the applied pressures and temperatures. A comparison of the saturation fluence with the thermodynamic condensation energy of the SDW state showed that the absorbed pump energy required for the suppression of the magnetic order largely exceeds the condensation energy, indicating that a large portion of the absorbed pump energy is transferred to the phonon bath. Using the parameters of the SDW relaxation process, we have estimated the variation of the SDW gap as a function of temperature and pressure. Our results demonstrate an apparent difference in the character of the thermally induced phase transition and the pressure-driven quantum phase transition. The former is first order and occurs rather abruptly near T_{SDW}, whereas the latter occurs gradually and the SDW gap starts to decrease for pressures well below the critical pressure p_{SDW}. This behavior suggests a second-order character of the quantum phase transition in $BaFe_2As_2$, in agreement with previous studies of quantum fluctuations in this material [9].

[1] Y. Kamihara, T. Watanabe, M. Hirano, and H. Hosono, Iron-based layered superconductor La[O$_{1-x}$F$_x$]FeAs ($x = 0.05 - 0.12$) with Tc = 26 K, J. Am. Chem. Soc. **130**, 3296 (2008).

[2] S. A. J. Kimber, A. Kreyssig, Y.-Z. Zhang, H. O. Jeschke, R. Valentí, F. Yokaichiya, E. Colombier, J. Yan, T. C. Hansen, T. Chatterji, R. J. McQueeney, P. C. Canfield, A. I. Goldman, and D. N. Argyriou, Similarities between structural distor-tions under pressure and chemical doping in superconducting BaFe$_2$As$_2$, Nat. Mater. **8**, 471 (2009).

[3] E. Colombier, S. L. Bud'ko, N. Ni, and P. C. Canfield, Com-plete pressure-dependent phase diagrams for SrFe$_2$As$_2$ and BaFe$_2$As$_2$, Phys. Rev. B **79**, 224518 (2009).

[4] Y. Nakai, T. Iye, S. Kitagawa, K. Ishida, H. Ikeda, S. Kasahara, H. Shishido, T. Shibauchi, Y. Matsuda, and T. Terashima, Unconventional Superconductivity and Antiferromagnetic

Quantum Critical Behavior in the Isovalent-Doped $BaFe_2(As_{1-x}P_x)_2$, Phys. Rev. Lett. **105**, 107003 (2010).

[5] S. Aswartham, M. Abdel-Hafiez, D. Bombor, M. Kumar, A. U. B. Wolter, C. Hess, D. V. Evtushinsky, V. B. Zabolotnyy, A. A. Kordyuk, T. K. Kim, S. V. Borisenko, G. Behr, B. Büchner, and S. Wurmehl, Hole doping in $BaFe_2As_2$: The case of $Ba_{1-x}Na_xFe_2As_2$ single crystals, Phys. Rev. B **85**, 224520 (2012).

[6] J.-H. Chu, J. G. Analytis, C. Kucharczyk, and I. R. Fisher, Determination of the phase diagram of the electron-doped superconductor $Ba(Fe_{1-x}Co_x)_2As_2$, Phys. Rev. B **79**, 014506 (2009).

[7] J. Paglione and R. L. Greene, High-temperature superconductivity in iron-based materials, Nat. Phys. **6**, 645 (2010).

[8] P. L. Alireza, Y. T. C. Ko, J. Gillett, C. M. Petrone, J. M. Cole, G. G. Lonzarich, and S. E. Sebastian, $SrFe_2As_2$ and $BaFe_2As_2$, J. Phys.: Condens. Matter **21**, 012208 (2009).

[9] S. Kasahara, T. Shibauchi, K. Hashimoto, K. Ikada, S. Tonegawa, R. Okazaki, H. Shishido, H. Ikeda, H. Takeya, K. Hirata, T. Terashima, and Y. Matsuda, Evolution from non-Fermi to Fermi-liquid transport via isovalent doping in $BaFe_2(As_{1-x}P_x)_2$ superconductors, Phys. Rev. B **81**, 184519 (2010).

[10] S. Sachdev and B. Keimer, Quantum criticality, Phys. Today **64**(2), 29 (2011).

[11] J. J. Wu, J. F. Lin, X. C. Wang, Q. Q. Liu, J. L. Zhu, Y. M. Xiao, P. Chow, and C. Jin, Pressure-decoupled magnetic and structural transitions of the parent compound of iron-based 122 superconductors $BaFe_2As_2$, Proc. Natl. Acad. Sci. U.S.A. **110**, 17263 (2013).

[12] J. Zhu, Z.-X. Yang, X.-Y. Hou, T. Guan, Q.-T. Zhang, Y.-Q. Li, X.-F. Han, J. Zhang, C.-H. Li, L. Shan, G.-F. Chen, and C. Ren, Tunneling spectroscopy of $Al/AlO_x/Pb$ subjected to hydrostatic pressure, Appl. Phys. Lett. **106**, 202601 (2015).

[13] L. Cao, W. Liu, G. Li, G. Dai, Q. Zheng, Y. Wang, K. Jiang, S. Zhu, L. Huang, L. Kong, F. Yang, X. Wang, W. Zhou, X. Lin, J. Hu, C. Jin, H. Ding, and H.-J. Gao, Two distinct superconducting states controlled by orientations of local wrinkles in LiFeAs, Nat. Commun. **12**, 6312 (2021).

[14] E. Uykur, T. Kobayashi, W. Hirata, S. Miyasaka, S. Tajima, and C. A. Kuntscher, Optical study of $BaFe_2As_2$ under pressure: Coexistence of spin-density-wave gap and superconductivity, Phys. Rev. B **92**, 245133 (2015).

[15] J. Demsar, Non-equilibrium phenomena in superconductors probed by femtosecond time-domain spectroscopy, J. Low Temp. Phys. **201**, 676 (2020).

[16] E. E. M. Chia, D. Talbayev, J.-X. Zhu, H. Q. Yuan, T. Park, J. D. Thompson, C. Panagopoulos, G. F. Chen, J. L. Luo, N. L. Wang, and A. J. Taylor, Ultrafast Pump-Probe Study of Phase Separation and Competing Orders in the Underdoped $(Ba, K)Fe_2As_2$ Superconductor, Phys. Rev. Lett. **104**, 027003 (2010).

[17] L. Stojchevska, P. Kusar, T. Mertelj, V. V. Kabanov, X. Lin, G. H. Cao, Z. A. Xu, and D. Mihailovic, Electron-phonon coupling and the charge gap of spin-density wave iron-pnictide materials from quasiparticle relaxation dynamics, Phys. Rev. B **82**, 012505 (2010).

[18] T. Mertelj, P. Kusar, V. V. Kabanov, L. Stojchevska, N. D. Zhigadlo, S. Katrych, Z. Bukowski, J. Karpinski, S. Weyeneth, and D. Mihailovic, Quasiparticle relaxation dynamics in spin-density-wave and superconducting $SmFeAsO_{1-x}F_x$ single crystals, Phys. Rev. B **81**, 224504 (2010).

[19] K. W. Kim, A. Pashkin, H. Schäfer, M. Beyer, M. Porer, T. Wolf, C. Bernhard, J. Demsar, R. Huber, and A. Leitenstorfer, Ultrafast transient generation of spin-density-wave order in the normal state of $BaFe_2As_2$ driven by coherent lattice vibrations, Nat. Mater. **11**, 497 (2012).

[20] S. Aswartham, C. Nacke, G. Friemel, N. Leps, S. Wurmehl, N. Wizent, C. Hess, R. Klingeler, G. Behr, S. Singh, and B. Büchner, Single crystal growth and physical properties of superconducting ferro-pnictides $Ba(Fe, Co)_2As_2$ grown using self-flux and Bridgman techniques, J. Cryst. Growth **314**, 341 (2011).

[21] A. Jayaraman, Diamond anvil cell and high-pressure physical investigations, Rev. Mod. Phys. **55**, 65 (1983).

[22] J. Demsar, K. Biljaković, and D. Mihailovic, Single Particle and Collective Excitations in the One-Dimensional Charge Density Wave Solid $K_{0.3}MoO_3$ Probed in Real Time by Femtosecond Spectroscopy, Phys. Rev. Lett. **83**, 800 (1999).

[23] N. Gedik, P. Blake, R. C. Spitzer, J. Orenstein, R. Liang, D. A. Bonn, and W. N. Hardy, Single-quasiparticle stability and quasiparticle-pair decay in $YBa_2Cu_3O_{6.5}$, Phys. Rev. B **70**, 014504 (2004).

[24] D. H. Torchinsky, G. F. Chen, J. L. Luo, N. L. Wang, and N. Gedik, Band-dependent quasiparticle dynamics in single crystals of the $Ba_{0.6}K_{0.4}Fe_2As_2$ superconductor revealed by pump-probe spectroscopy, Phys. Rev. Lett. **105**, 027005 (2010).

[25] L. Stojchevska, T. Mertelj, J.-H. Chu, I. R. Fisher, and D. Mihailovic, Doping dependence of femtosecond quasiparticle relaxation dynamics in $Ba(Fe, Co)_2As_2$ single crystals: Evidence for normal-state nematic fluctuations, Phys. Rev. B **86**, 024519 (2012).

[26] D. H. Torchinsky, J. W. McIver, D. Hsieh, G. F. Chen, J. L. Luo, N. L. Wang, and N. Gedik, Nonequilibrium quasiparticle relaxation dynamics in single crystals of hole- and electron-doped $BaFe_2As_2$, Phys. Rev. B **84**, 104518 (2011).

[27] V. V. Kabanov, J. Demsar, B. Podobnik, and D. Mihailovic, Quasiparticle relaxation dynamics in superconductors with different gap structures: Theory and experiments on $YBa_2Cu_3O_{7-\delta}$, Phys. Rev. B **59**, 1497 (1999).

[28] P. Kusar, V. V. Kabanov, J. Demsar, T. Mertelj, S. Sugai, and D. Mihailovic, Controlled Vaporization of the Superconducting Condensate in Cuprate Superconductors by Femtosecond Photoexcitation, Phys. Rev. Lett. **101**, 227001 (2008).

[29] A. Schmid and G. Schön, Linearized kinetic equations and relaxation processes of a superconductor near T_c, J. Low Temp. Phys. **20**, 207 (1975).

[30] I. Schuller and K. E. Gray, Experimental Observation of the Relaxation Time of the Order Parameter in Superconductors, Phys. Rev. Lett. **36**, 429 (1976).

[31] See Supplemental Material at http://link.aps.org/supplemental/10.1103/PhysRevB.108.035101 for pump-probe data taken at a pressure of 4.4 GPa; the fluence dependence of the the signal; a discussion of the pressure-induced SDW transition, and the nature of the high pressure phase.

[32] M. Rotter, M. Tegel, D. Johrendt, I. Schellenberg, W. Hermes, and R. Pöttgen, Spin-density-wave anomaly at 140 K in the ternary iron arsenide $BaFe_2As_2$, Phys. Rev. B **78**, 020503(R) (2008).

[33] N. Barišić, D. Wu, M. Dressel, L. J. Li, G. H. Cao, and Z. A. Xu, Electrodynamics of electron-doped iron pnictide superconductors: Normal-state properties, Phys. Rev. B **82**, 054518 (2010).

[34] A. Lucarelli, A. Dusza, F. Pfuner, P. Lerch, J. G. Analytis, J.-H. Chu, I. R. Fisher, and L. Degiorgi, Charge dynamics of Co-doped $BaFe_2As_2$, New J. Phys. **12**, 073036 (2010).

[35] M. Yi, Y. Zhang, Z.-K. Liu, X. Ding, J.-H. Chu, A. Kemper, N. Plonka, B. Moritz, M. Hashimoto, S.-K. Mo, Z. Hussain, T. Devereaux, I. Fisher, H. Wen, Z.-X. Shen, and D. Lu, Dynamic competition between spin-density wave order and superconductivity in underdoped $Ba_{1-x}K_xFe_2As_2$, Nat. Commun. **5**, 3711 (2014).